Numerical Solution of the Downwash Associated with a Blown-Flap System

Eric Loth*
and
Barnes W. McCormick†
The Pennsylvania State University, University Park, Pennsylvania

For blown-flap aircraft, large downwashes typically occur downstream of the wing due to the high downward momentum of the lifting jet. To determine the velocities induced by the wing- and jet-flap circulation, a three-dimensional, nonlinear, finite-element model that can predict downwash angles at any desired location has been developed. Vortex lattices positioned on the wing, flap, and thin jet sheet provide vortex filaments and control points to satisfy kinematic and dynamic boundary conditions. To simplify the mixed-boundary value problem and to reduce computer run time, the rollup of the wake in the spanwise direction has been neglected. In addition, the spanwise distribution of circulation in the wake is assumed to be elliptic in form. A reasonably fast and stable iterative method that allowed a self-consistent wake path to be found was used. Predicted downwash and lift coefficients generally agree with experimental values for various test conditions; but further improvements, such as fuselage modeling, might enhance the accuracy of the model.

Nomenclature

AR = wing aspect ratio
C = airfoil chord length
C_f/C = flap chord ratio
C_j = blowing coefficient
C_r = root chord length
CX = velocity induced in the x direction due to a unit vorticity
F_i = turning force of jet in radial direction
m_j = jet mass flow rate over blown flap
M = number of chordwise wing lattice divisions
S = total wing area
S' = equivalent blown wing area
V = freestream velocity
V_j = velocity of blown jet
V_t = average tangential velocity surrounding the blown jet
V_x = velocity in the x direction due to the wing lattice
V_{xw} = velocity in the x direction due to the wake lattice
V_z = velocity in the z direction due to the wing lattice
V_{zw} = velocity in the z direction due to the wake lattice
x = distance in the downstream direction parallel with the freestream
y = distance along the wing span
y_f = extent of blown flap along the wing span
z = distance in the vertical direction
α = wing angle of attack
δ = initial jet deflection angle
ϵ = downwash angle
γ = turning vorticity on wake lattice
γ_0 = centerline magnitude of turning vorticity
Γ = horseshoe vortex on wing lattice
λ = wing taper ratio
ρ = air density
θ = angle of wake sheet

Subscripts

k = pertaining to control point k
p = pertaining to horseshoe vortex p
r = pertaining to radial component
t = pertaining to tangential component

Presented as Paper 86-0473 at the AIAA 24th Aerospace Sciences Meeting, Reno, NV, Jan. 6–9, 1986; received Jan. 21, 1986; revision received Sept. 16, 1986. This paper is declared a work of the U.S. Government and is not subject to copyright protection in the United States.

*Graduate Assistant, Aerospace Engineering Department. Member AIAA.
†Boeing Professor, Aerospace Engineering Department. Fellow AIAA.

Introduction

THERE has been a growing interest in aircraft that may takeoff and land within short runway lengths. A jet-flapped wing is one technique used to provide the high lift coefficients necessary. The upper surface blown flap (USB) is a derivative of the internally blown jet flap (IBF) and generally utilizes the exhaust from engines mounted above the wing as the source for the blowing. The USB configuration (presented in Fig. 1) has emerged as a viable lift augmentation system that may be applied in future aircraft.

Because of the importance of aircraft stability and control at low flight speeds, a method is needed to describe the downstream flow angles. The large downwash angles associated with jet flaps can cause loss of tail effectiveness, and therefore are potentially dangerous. This paper presents a reasonably efficient and accurate numerical method to predict these angles based on simplifying, but plausible, assumptions. Details of the analysis, program logic, and results are presented in a thesis by the author.[1]

Previous Experimental Research

Past experimental work on the jet flap has focused primarily on measuring pressure and velocity distributions near the jet exit or on the wing surface. In comparison, the measurement and prediction of downstream downwash angles have received much less emphasis.

In general, a jet exits at some initial angle to a uniform crossflow, and its momentum is deflected in the direction of the freestream due to the impinging freestream momentum. The deflecting force provides the "jet turning" vorticity (depicted in Fig. 2) which is similar in direction and effect as the bound vorticity of a wing. The turning vorticity of a jet-flapped wing provides an additional induced lift known as

supercirculation. For finite jet widths, there is also trailing vorticity due to the shedding of the jet turning vorticity. The effect of this is similar to the trailing vortices of a finite wing.

One of the earlier experimental studies on jet-flapped finite wings using a finite semiwing model equipped with an IBF flap was conducted by Vogler.[2] Lift coefficients and downwash angles were obtained at various downstream distances and vertical locations for a range of blowing coefficient values.

Finite wing IBF downwash angle data were also obtained in wind tunnels by Alexander and Williams,[3] as well as by Butler et al.[4] As with the Vogler measurements, downwash angles were found by these investigators to be as high as 20 deg, even at high tail positions. In addition, Stewart has recently published experimental research on a wing/canard STOL configuration model with a finite IBF wing, including downwash angle measurements.[5]

Previous Theoretical and Numerical Studies

In 1956, Spence derived a linear, two-dimensional, incompressible model for a wing with a pure jet flap.[6] In this analytical treatment, the wing and jet vorticity were placed along the chord line. While nonlinear boundary conditions were maintained, only perturbations of the velocity in the z direction were allowed. Spence's solution for lift, moment, and vorticity distribution has compared favorably with two-dimensional experiments. Even for jet deflection angles as large as 60 deg, where one would expect the linear theory to break down, the prediction still produces reasonably good results. Spence's model has become the classic two-dimensional treatment of the jet flap.

Other linearized models that describe the three-dimensional wing lift and moment characteristics for the jet flap have followed with acceptable results. However, in their discussion of the problem, Williams et al.[7] point out that linearized theory is inadequate to accurately predict downwash angle behavior for large blown jet momentums.

Much analytical progress has been made within the last 15 years due to the availability of high-speed digital computers. Many researchers have used numerical treatments to solve STOL jet/wing problems with greater detail and accuracy. Among other advantages, computational studies have allowed researchers to let vorticity placement coincide with the deflected jet path when simulating the flowfield. Using vortex panel and lattice methods, many numerical models have successfully predicted the effects of jet blowing on wing lift and moment coefficients, as well as pressure, vorticity, and velocity distributions on and near the exiting surface.

For these cases, spanwise deformation of the wake is frequently neglected, jet curvature is based on the midspan wake deflection, and only the induced velocities in the z direction are examined. Many researchers have avoided the convergence problems of jet path position by employing empirical relations.

Wooler's numerical study for a delta wing with a lifting jet uses a series of horseshoe vortices on the jet sheet and is typical of computational setups.[8] Wooler stated that the agreement with experimental work "is quite good, except in the wake downstream of the jet, where the results differ considerably." The failure to accurately model the downstream flow is representative of the numerical models reviewed and indicates that a downwash model, such as that proposed herein, must consider the wake boundary conditions carefully.

Computational Model Description

General Overview

Jet-flap models, which have successfully determined the vorticity and pressure distributions on the wing, have focused generally on the interaction mechanism between the exiting surface and the jet. For the present investigation, however, the emphasis is shifted to modeling both the proper position and the strength of the downstream vorticity. However, by placing the wake vorticity on a self-consistent jet path, the task of providing a purely analytic closed-form solution becomes unreasonable.

A simple potential flow model that assumes an infinitely thin jet sheet has been developed. A three-dimensional distribution of vortex filaments defines the harmonic function that satisfies the mixed-boundary value problem. The numerical model allows the vorticity to be deflected along a force-free jet path using velocity perturbations in both the x and z directions, without small angle approximations. The present code can also handle a range of aircraft speeds for the cases of full or partial span jet flaps (either pure or hinged), as well as describing aspect ratio, sweep, taper, camber, twist, and ground effect.

One of the limitations of the model is that the jet sheet is flat in the spanwise direction and is therefore described by boundary conditions applied at the centerline. These assumptions greatly simplify the calculations needed: a free wake computational analysis would be highly time consuming. Silverstein et al.[9] concluded that it is usually sufficiently accurate to "take into account the wake distortion simply by considering the entire vortex sheet to be displaced vertically by an amount equal

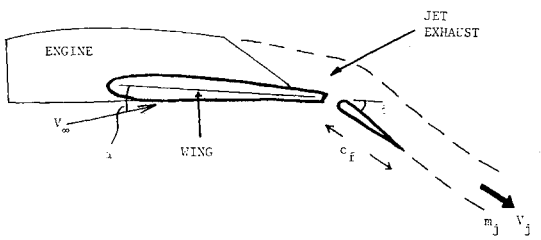

Fig. 1 Sketch of upper surface blown airfoil (USB).

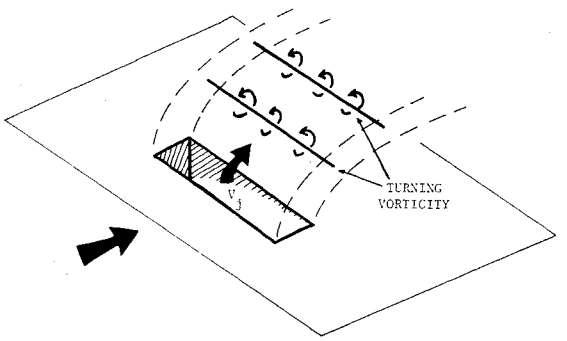

Fig. 2 Sketch of jet turning vorticity; air blown from rectangular opening into a crossflow.

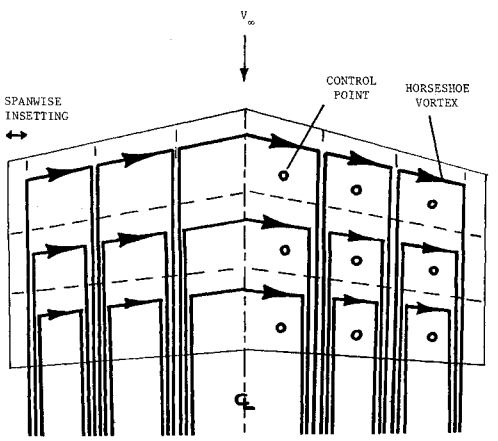

Fig. 3 Horseshoe vortex lattice over a nonflapped wing; wing contains $N \times M$ control points and $2 \times N \times M$ horseshoes ($N=3$, $M=3$).

to the displacement of the centerline of the actual distorted sheet" for downwash calculations behind unblown wings. This supports the choice to place the boundary conditions along the symmetric wake centerline. Finally, no attempt has been made to model viscous effects such as skin-friction drag over the upper flap surface, flow separation, or vortex core simulation.

Kinematic boundary conditions satisfied on the wing and jet path assure that the normal velocity at the wing surface and along the wake centerline is zero. The dynamic boundary condition is satisfied along the wake centerline by relating the incremental deflection of the jet momentum with local turning vorticity. Simultaneously satisfying these boundary conditions results in a self-consistent modeling of the wake shape. Once the distribution of the vorticity in both strength and position is known, the steady-state downwash may be calculated directly at any point.

The Wing Lattice

A system of horseshoe vortices placed over the wing surface is a common and accepted finite-element approach that provides an accurate vorticity distribution (see Fig. 3). The positioning of control points and vortex filaments is based on the Weissinger approach for a finite wing. The chordwise and spanwise distribution ($M\times N$) of vortex elements over unflapped and flapped portions of the wing is determined by the user.

Hough discusses ways to optimize the use of a wing lattice.[10] The recommendations used in the present model include 1) one-quarter lattice insetting at the wing tips to accelerate convergence as the number of spanwise elements increased; 2) horseshoe filaments that are twisted, tapered, swept, and flapped according to the aircraft geometry to properly position the vortex distribution; 3) placing the bound vortex filaments along discontinuities, such as the flap hinge line and the trailing edge, for the blown-flap case; and 4) arranging the lattice such that resolution is highest on the flap surface and near the trailing edge.

On the wing, each control point k is used to satisfy the kinematic condition that the flow be parallel with the local wing camberline angle. Using the Biot-Savart relation for a vortex filament, the velocities V_x and V_z induced by the wing in the x and z directions, and the corresponding velocities V_{xw} and V_{zw} induced by the wake can be found at any point. Therefore, the boundary conditions will be satisfied when

$$\tan(\alpha_k)=\frac{V_z+V_{zw}}{V_\infty+V_x+V_{xw}} \tag{1}$$

where

$$V_x\boldsymbol{i}+V_z\boldsymbol{j}=\sum_{p=1}^{N\times M}\int\frac{\Gamma_p\boldsymbol{r}\times d\boldsymbol{w}_p}{4\pi|\boldsymbol{r}|^3} \tag{2}$$

Here, $\boldsymbol{r}$ is the vector from control point k to the filaments which comprise the horseshoe vortex of strength Γ_p, and the vector $d\boldsymbol{w}_p$ is the differential length of the horseshoe vortex filament. The wake velocities V_{xw} and V_{zw} are similarly defined based on the vortex filaments distributed in the wake lattice.

The Biot-Savart rule for a differential vortex element in vector form was integrated to provide the capability of calculating the induced velocity due to any system of finite and semi-infinite vortex line segments. Ground effect was modeled by including a mirror image of each vortex segment placed at an equal distance below the ground plane.

In terms of the $N\times M$ system of equations, the array of wing horseshoe strengths Γ_p can be expressed as functions of the velocity components

$$[CZ]_{k,p}\times[\Gamma]_p+[V_{zw}]_k=[\tan\alpha]_k([CX]_{k,p}\times[\Gamma]_p+[V_\infty]+[V_{xw}]) \tag{3}$$

where $k=1, N\times M$ and $p=1, N\times M$ and $CX_{k,p}$ and $CZ_{k,p}$ are the x and z components of velocity induced at control point k

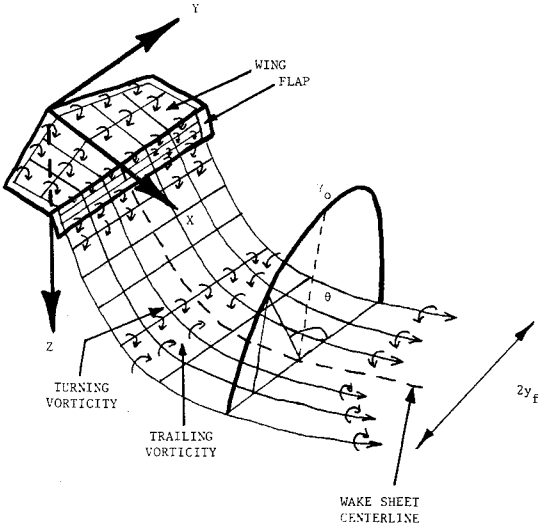

Fig. 5 Sketch of computational model for a wing and jet lattice; turning vorticity has an elliptic distribution.

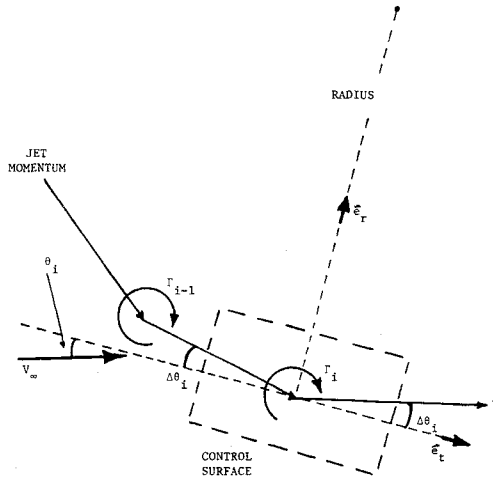

Fig. 4 Sketch of turning vorticity for an incremental jet element.

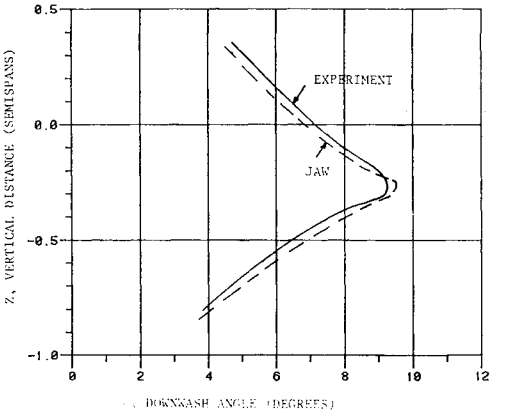

Fig. 6 Downwash profile for U.S. 45 tapered wing; downwash measured 1.15 semispans behind quarter-chord for $S=46$ ft, $\mathcal{R}=6$, $C_L=1.35$, and $\lambda=0.5$.

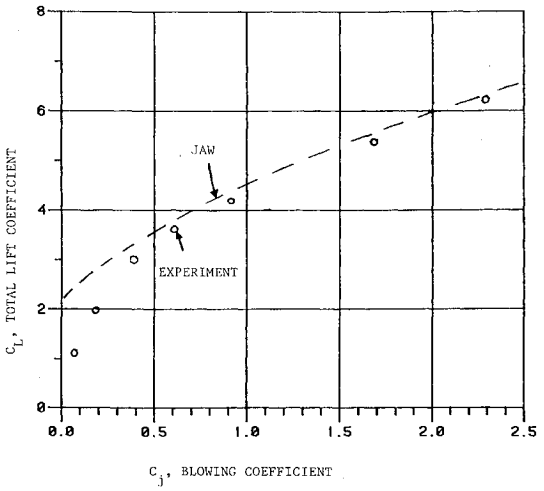

Fig. 7 Vogler lift coefficient for rectangular wing; $\mathcal{R}=7.6$, $C_f/C=0.125$, and $\delta=55$ deg.

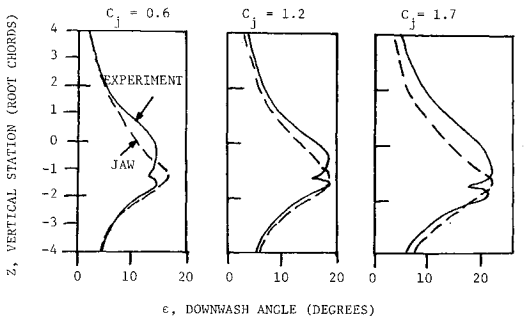

Fig. 8 Vogler downwash profiles for various blowing coefficients; downwash at 50% semispan station and three chord lengths downstream for $\mathcal{R}=7.6$, $C_f/C=0.125$, and $\delta=55$ deg.

due to wing horseshoe vortex p with a unit strength of vorticity. The summation of the trailing velocities at the trailing edge determines the initial trailing vorticity of the wake sheet. Using matrix inversion instead of Gaussian elimination significantly reduces computer time.

The Jet Turning Vorticity

In addition to the wing trailing vorticity, the turning vorticity associated with jet curvature must be found for the wake lattice. The deflected wake is represented by a lattice of connected finite length segments beginning at the flap trailing edge and eventually extending infinitely downstream. The elements are placed parallel to the local velocity vector calculated at the symmetric centerline for each path junction.

By isolating a small spanwise element of curved jet with a control surface, as shown in Fig. 4, the integral form of the jet momentum equations can be found using the momentum theory. Using the Kutta-Joukowski relation, the induced force F_1, due to a vortex filament placed at the deflection junction, is equated with the force required to turn the jet momentum through the deflection angle $\Delta\theta_i$

$$F_i=\frac{\mathrm{d}}{\mathrm{d}t}\,(\text{jet momentum})_i\simeq(m_jV_j)2\Delta\theta\boldsymbol{e}_r \tag{4}$$

$$\boldsymbol{F}_i=\int_{-yf}^{+yf}\rho\boldsymbol{V}\times\boldsymbol{\gamma}\mathrm{d}y \tag{5}$$

where y_f is the semispan extent of the blown flap.

It is assumed that the flow velocity surrounding the jet sheet is constant in the spanwise direction and is incompressible. Next, the vorticity across the span of the jet sheet is assumed to be elliptically loaded. This is the distribution used in slender wing theory. Many researchers, such as Maskell and Spence,[11] as well as Thomas and Ross,[12] have also successfully applied such an elliptic distribution for the jet vorticity to predict wing aerodynamic characteristics. An arbitrary spanwise distribution, as used on the wing, should be more accurate; however, the elliptic assumption significantly reduces computer run time and model complexity.

The expression for the turning vorticity γ as a function of spanwise distance y then becomes

$$\gamma=\gamma_0\sin\beta \text{ where } \beta=\cos^{-1}(-y/yf) \tag{6}$$

where γ_0 is the centerline magnitude of vorticity. Note that the vorticity will be a maximum at the centerline and go to zero on either edge of the sheet. Using the prescribed vorticity distribution, γ_0 becomes a local function of the junction velocity V_t and the defection angle $\Delta\theta$

$$\gamma=(2C_jS'\Delta\theta)/(C_r\pi y_fV_t) \tag{7a}$$

where

$$C_j=(2m_jV_j)/(\rho_\infty V_\infty^2C_r) \tag{7b}$$

S' is the wing span based on the flown portion, and C_r is the root chord length.

$$V_t=\cos_i(V\infty+V_x+V_x+V_{xw})+\sin\theta_i(V_z+V_{zw}) \tag{8}$$

Jet and Wing Combination

The wake and wing are combined to form a three-dimensional lattice composed of vortex filaments and control points, where symmetry is assumed along the midspan. The vortex sheet begins at an initial jet deflection angle and then continues along the midspan streamline of the wake for MEND number of finite length segments.

At each of the wake junctions, the turning vorticity is distributed elliptically over the jet span, as shown in Fig. 5. The boundary conditions imposed at the centerline of the symmetric wake lattice mandate a zero normal velocity component and a net turning vorticity distribution that agrees with the wake junction angle. The element of the wake in the x direction is set up once and remains fixed; whereas the deflection in the z direction varies iteratively. In order to provide proper resolution, the length of the x increments in the jet lattice vary and are smallest near the wing trailing edge.

Combining the trailing vortices of the wing and the wake vortices along the jet lattice by the Helmholtz theorem, the entire flowfield can be described. The downwash angle ϵ can then be calculated at any point by summing the induced velocities due to all vortex filaments in the wing and wake lattice

$$\epsilon=\frac{\Sigma(V_z+V_{zw})}{\Sigma(V_\infty+V_x+V_{xw})}$$

The general logic of the program is to solve the system of equations for the zero-blowing case, increment the blowing coefficient, and iterate to find a self-consistent solution for this new blowing coefficient. This process is repeated until the desired blowing coefficient is reached. For each of the converged flowfields, the lift coefficient and downwash are calculated.

The first wing solution assumes no wake deflection in solving for the initial horseshoe strengths. Based on this, a wake path is created by marching down the centerline of the sheet (element by element) and by satisfying the kinematic boundary condition. At each control point located at the segment junctions, the induced velocity due to the wing and wake is com-

puted and added to the freestream velocity. Using the locally predicted velocity slopes found at two successive control points, the deflected coordinate Z of each new segment can be determined. Due to the path's high sensitivity to small changes in turning vorticity, instability of the wake path was avoided by damping out the turning vorticity (using the previous iteration values).

Convergence is reached if the maximum change between path iterations for all wake sections does not exceed some specified percentage, typically 1%. If the path is not converged, the system is iterated by placing the wing trailing vortices along the new wake shape. Using this updated vorticity placement, the wake induced velocity is found for each of the wing control points; the wing lattice is resolved from this. The scheme is similarly repeated until the shape converges.

Jet and Wing Code Results and Comparisons

No Blowing Results

Predictions by jet and wing (JAW) lattice code for lift coefficient and downwash angles for arbitrary wing configurations compared well with experimental results. Generally, a wing lattice of eight spanwise elements and seven chordwise elements (for the case with flaps) provided a sufficient vorticity resolution.

The input parameters of twist, taper, sweep, and aspect ratio were all varied with favorable correlation for lift coefficients from linearized theory. The predicted downstream downwash profile of a tapered wing with a U.S. 45 airfoil showed good agreement with tested values by Silverstein et al. (see Fig. 6), as did other comparisons with unflapped wing measurements. The predicted position of the wake path was found to lie at an approximate average spanwise deflection of an actual finite wing wake rollup. However, lift and downwash measurements for high flap angle studies were overpredicted by the JAW code due to the neglect of flow separation.

Blown Flap Results

Once confidence in the zero-blowing case had been achieved, the code was modified to include jet momentum effects. Using the variable step size along the wake path, about a dozen elements in the x direction are required to define the jet shape. Computer run times on DEC VAX 11/780 were generally less than 10 min for cases of $C_j = 2$, using a blowing coefficient of 0.5. For a typical increment of the blowing coefficient, four to seven path iterations are required for convergence, based on a maximum path change criteria of 1%. Converged net jet turning vorticity strengths were verified by integrating the lift force due to this vorticity and comparing it with the force due to the overall jet momentum deflection.

The JAW code shows good agreement for lift coefficients with Spence's linear relations, modified to include finite wing effects. The close comparison suggests that the linearized relations used at even moderately high angles are a good approximation for lift values.

Vogler's[2] wind-tunnel tests were one of the four experimental downwash studies used for comparison with the numerical code. The aircraft test model used was a semibody with an untwisted rectangular wing of aspect ratio 7.6. The lift curves for the jet blown flap that were deflected 60 deg compared favorably to values predicted by the present code (see Fig. 7). Downstream downwash values obtained for various blowing coefficients (Fig. 8) and vertical locations (Fig. 9) by Vogler were compared to JAW predicted values, with good correlation even at the wing tip spanwise station. All measurements were taken with a flow angle probe placed three chord lengths downstream of the quarter chord line.

Williams and Alexander[3] tested a half-body with a rectangular wing of aspect ratio 6 and full span blown flaps. The wing-tunnel measurements for lift agree reasonably well with predicted values for flap deflection angles of 30 and 60 deg, as seen in Fig. 10. The experimental downwash data obtained at

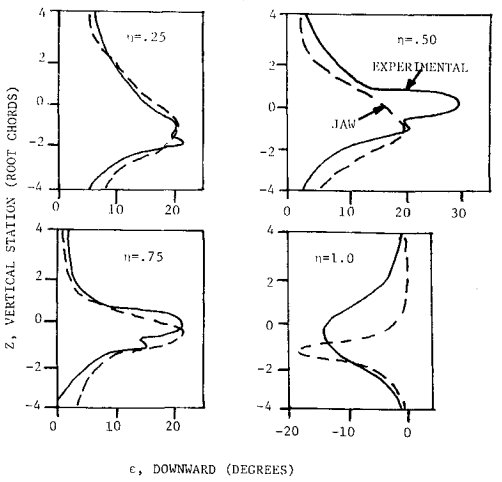

Fig. 9 Vogler downwash profile for various spanwise stations; downwash at three chord lengths downstream of quarter chord line for $\mathcal{R} = 7.6$, $C_f/C = 0.125$, $C_j = 1.7$, and $\delta = 55$ deg.

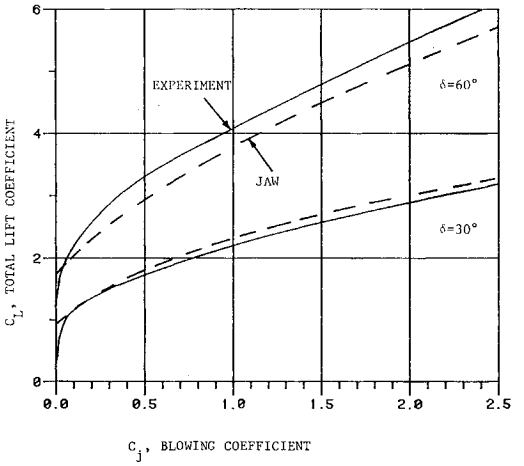

Fig. 10 Lift coefficients for Williams rectangular wing for $\mathcal{R} = 6$ and $C_f/C = 0.1$, with 12% thick RAE 104 airfoil.

three chord lengths downstream for three vertical stations were accurately predicted by the JAW code (see Fig. 11). Downwash comparisons as a function of blowing coefficient also showed good agreement (see Fig. 12). As expected, for the small C_j value of 0.1, the neglect of separation effects results in overprediction of lift coefficients and downwash angles by the JAW code.

Butler et al.[4] used a complete airplane model with a moderately tapered and swept wing of aspect ratio 9. For the jet angle of 52 deg, good correlation with the JAW predicted results is found for the experimental lift coefficients and downwash angles.

The fourth and most recent study was conducted with a canard VSTOL configuration model by Stewart[5] at NASA Langley Research Center. The highly tapered and swept wing of aspect ratio 2.12, combined with a fuselage section that covered one-fifth of the total wing span and a ground board height of less than two root chords, represents an extreme case to test the applicable range of the analytical mode. Predicted lift coefficients exhibited adequate (but not accurate) comparison with the measured values. However, the downwash angles predicted by the JAW code were significantly less than the experimental values; at high injection angles and blowing coefficients, the predictions were as little as half of the experimental downwash angles.

There may be several reasons for this poor downwash correlation. The neglect fuselage interference effects may be

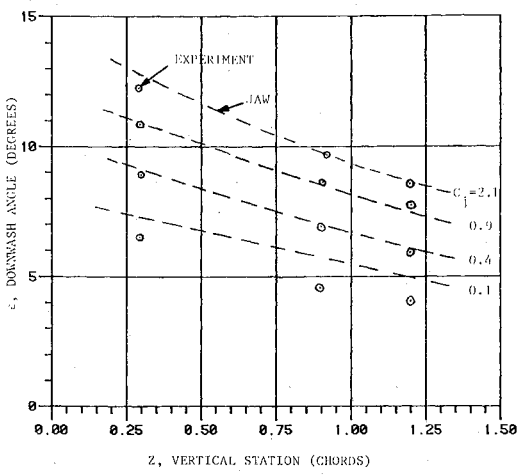

Fig. 11 Williams downwash at various vertical stations for $\mathcal{R}=6$, $C_f/C=0.1$, and $\delta=60$ deg.

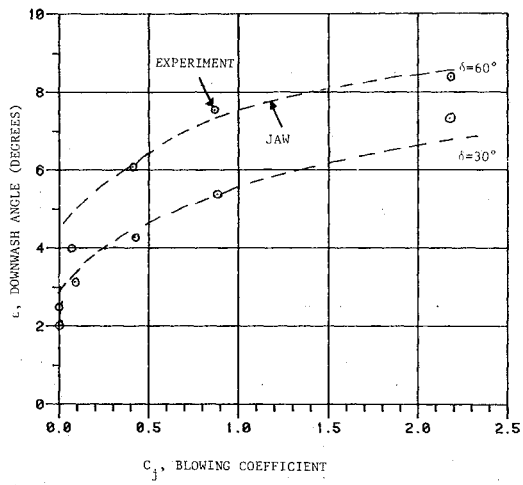

Fig. 12 Williams downwash for various blowing coefficients for $\mathcal{R}=6$ and $C_f/C=0.1$.

significant due to the large relative size of the fuselage as compared to the wing. In the wind-tunnel testing, the low ground clearance of the test model may have caused large standing vortices not predicted by the JAW code. And finally, the high sweep angle of the aircraft model may be too large to reasonably apply such a lattice model. Additional experimental testing for this wing/canard model, which may include a rake study of the downwash angles, is anticipated; this might help pinpoint the problem of predicting the downwash for this configuration.

As expected, the lift coefficient was found to slightly increase, and the downwash angles were found to slightly decrease, near the ground. Butler noted that, in the presence of ground heights less than five chord lengths, the downwash began to be measurably affected by ground effect; this trend was also found with the JAW code. When the ground effect was taken into account, the computer run time was increased by as much as a factor of two, and sometimes wake instabilities required relaxation of the path deflection coordinates.

Lift coefficients, jet trajectories, and downwash angles are not predicted with acceptable accuracy for initial jet angles of 80 deg or more. This is because the viscous effects begin to dominate, and the potential model is not expected to accurately apply to such flows. The same is true for the case of high wing or flap angles with no blowing, where neglect of separation leads to an overestimation of experimental lift downwash values. Obviously, care must be taken to insure that the inviscid features are dominant when employing the present code.

Conclusions

A nonlinear, self-consistent jet wake model has been formulated using a vortex lattice on the wing and jet sheet. The purpose of this model is to calculate induced velocities in the surrounding flowfield. Although this steady-state wake model neglects wake roll up and is thus not applicable close to the wing, it is believed to be relatively accurate in calculating downwash angles at points removed from the jet wake. Convergence was found to be reasonably fast and stable for a proper increment of the blowing coefficient.

The numerical results for the various design configuration compared favorably with experimental results and linear analytic models. As expected, for unblown flaps, the neglect of separation resulted in an overprediction of lift and downwash by the model. Other differences can be attributed to 1) the effect of wing thickness, 2) the experimental uncertainty of the initial jet angle, and 3) the fuselage interference effects.

The downwash correlation was good, even for three separate experiments that used moderately high blowing and initial jet angles. However, the code did not show good agreement when compared with Stewart's data; this discrepancy may be due to high sweep, fuselage interference, or ground effects.

Although accuracy is lost for flowfields where viscous effects begin to dominate, the code is believed to be well suited for preliminary design use to calculate downwash angles, as well as to provide approximate wing lift distributions.

Acknowledgments

This reseach was sponsored by Naval Air Development Center, under Contract N62269-84-C-0437, entitled "A Study of Downwash Associated with High-Lift Systems," under the technical direction of Marvin Walters.

References

[1]Loth, E., "A Numerical Solution of the Downwash Associated with a Blown Flap System," M.S. Thesis, The Pennsylvania State University, University Park, PA, Dec. 1985.

[2]Vogler, R. D. and Turner, T. R., "Wind-Tunnel Investigation at Low Speeds to Determine Flow-Field Characteristics and Ground Influence on a Model with Jet Augmented Flaps," Langley Aeronautical Laboratory, NASA TN-4116, Sept. 1957.

[3]Alexander, A. J. and Williams, J., "Wind-Tunnel Experiments on a Rectangular-Wing Jet-Flap Model of Aspect-Ratio 6," ARC R&M 3329, 1964.

[4]Butler, S. J. F., Guyett, M. B., and Moy, B. A., "Six-Component Low-Speed Wind Tunnel Test of Jet-Flap Complete Models," Unpublished M.O.A. Report (mentioned in Ref. 2).

[5]Stewart, V. R., "Aerodynamic Characteristics of a Propulsive Wing/Canard Concept at STOL Speeds–Interim Report," Rockwell International, NADC CR-177982, Nov. 1985.

[6]Spence, D. A., "Lift of a Thin Jet-Flapped Wing," *Proceedings of the Royal Aeronautics Society*, A-238, 1956, pp. 46–68.

[7]Williams, J., Butler, S. J. F., and Wood, M. N., "The Aerodynamics of Jet Flaps," ARC R&M 3304, 1963.

[8]Wooler, P. T., "Development of an Analytic Model for the Flow of a Jet into a Subsonic Crosswind," NASA SP-218, Sept. 1969, pp. 101-118.

[9]Silverstein, A., Katzoff, S., and Bennet, W. K., "Downwash and Wake Behind Plain and Flapped Airfoils," NASA TN-651, 1939.

[10]Hough, G. R., "Remarks on Vortex Lattice Arrangements," *Journal of Aircraft*, Vol. 10, No. 5, May 1973, pp. 314–317.

[11]Maskell, E. C. and Spence, D. A., "A Theory of the Jet Flap in Three-Dimensions," *Proceedings of the Royal Aeronautics Society*, A251, 1959, pp. 407-425.

[12]Thomas, H. H. B. M. and Ross, A. J., "The Calculation of the Rotary Lateral Stability Derivatives for a Jet-Flapped Wing," ARC R&M 3277, 1958.